PERGAMON

International Journal of Heat and Mass Transfer 46 (2003) 149–159

International Journal of HEAT and MASS TRANSFER

www.elsevier.com/locate/ijhmt

# Size effect on microscale single-phase flow and heat transfer

Zeng-Yuan Guo *, Zhi-Xin Li

*Department of Engineering Mechanics, Tsinghua University, Beijing 100084, China*

Received 16 March 2002

**Abstract**

The present discussion will focus on the size effect induced by the variation of dominant factors and phenomena in the flow and heat transfer as the device scale decreases. Due to the larger surface to volume ratio for microchannels and microdevices, factors related to surface effects have more impact to microscale flow and heat transfer. For example, surface friction induced flow compressibility makes the fluid velocity profiles flatter and leads to higher friction factors and Nusselt numbers; surface roughness is likely responsible for the early transition from laminar to turbulent flow and the increased friction factor and Nusselt number; the relative importance of viscous force modifies the correlation between *Nu* and *Ra* for natural convection in a microenclosure and, other effects, such as channel surface geometry, surface electrostatic charges, axial heat conduction in the channel wall and measurement errors, could lead to different flow and heat transfer behaviors from that at conventional scales.


*Keywords:* Microscale flow and heat transfer; Single phase; Size effect

## 1. Introduction

Microelectromechanical systems (MEMS) are having an important impact in medicine and bioengineering, information technologies and other industries, so MEMS research is widely spread, especially for basic and applied research on fluid flow and heat transfer at microscales. Some analytical and experimental results for the flow and heat transfer characteristics in small/microchannels are remarkably different from those for conventional size channels, such as the variation of the friction factor, the heat transfer coefficient and the early transition from laminar to turbulent flow. Large differences exist in the reported friction factor and the heat transfer coefficients for single-phase flow through channels, and in the reported Reynolds numbers ($300 < Re_c < 2300$) for transition from laminar to turbulent flow in microscale passages. For example, Wu and Little [1] measured the friction factors for flow of gas (nitrogen, argon and hydrogen) in very fine channels used for refrigerators, the product of the friction factor and the Reynolds number ($f\,Re$) was as large as 118, which is much larger than the value of 64 for the laminar flow in conventional channels. Pfahler et al. [2,3] conducted a series of experimental studies with gases ($N_2$, He) and liquids (isopropyl and silicone oil) flowing through microchannels, the measured friction factors were consistently lower than the theoretical predictions and decreased with decreasing Reynolds number for laminar flows in the small Reynolds number regime. Choi et al. [4] measured the friction factors for nitrogen gas flow in microtubes for both the laminar and turbulent regimes. For Reynolds numbers smaller than about 400, the friction factor correlation had a value for the constant $C = f\,Re = 53$, instead of 64. Papautsky and coworkers [5,6] conducted experiments for water flow. The normalized friction coefficient $C$ for the experimental data was found to be approximately 1.12 for large $Re$ and 1.2 for small $Re$. Wang and Peng [7] reported single-phase heat transfer coefficients in six rectangular channels having $0.31 < D_h < 0.75$ mm for water and methanol. Their Nusselt numbers were only 35% of those predicted

* Corresponding author. Tel.: +86-10-62782660; fax: +86-10-62781610.

*E-mail addresses:* demgzy@tsinghua.edu.cn (Z.-Y. Guo), lizhx@tsinghua.edu.cn (Z.-X. Li).

0017-9310/03/$ - see front matter 
PII: S0017-9310(02)00209-0

**Nomenclature**

| | |
|---|---|
| $a$ | thermal diffusivity ($m^2/s$); side length of square or equilateral triangle microchannels (m) |
| $C$ | friction constant |
| $d$ | tube diameter (m) |
| $d_i$ | inner diameter (m) |
| $D_h$ | hydraulic diameter (m) |
| $Ec$ | Eckert number |
| $f$ | friction factor |
| $f'$ | friction factor with effect of gas bubble |
| $g$ | gravitational acceleration ($m/s^2$) |
| $Gr$ | Grashof number |
| $h$ | heat transfer coefficient ($W/m^2\,K$) |
| $k$ | thermal conductivity (W/mK) |
| $Kn$ | Knudsen number |
| $l$ | length (m) |
| $L$ | length (m) |
| $m$ | mass flow rate (kg/s) |
| $M$ | Mach number |
| $M_0$ | inlet Mach number |
| $M_{loc}$ | local Mach number |
| $M_m$ | average Mach number of inlet and outlet |
| $Nu$ | Nusselt number |
| $p$ | pressure (Pa), perimeter (m) |
| $Pr$ | Prandtl number |
| $r$ | radial coordinate; radius (m) |
| $R^*$ | ratio of outer to inner diameters |
| $Ra$ | Rayleigh number |
| $Re$ | Reynolds number |
| $T$ | temperature (K) |
| $U$ | dimensionless axial velocity |
| $x$ | coordinate |

*Greek symbols*

| | |
|---|---|
| $\beta$ | volume expansion coefficient (1/K) |
| $\mu$ | dynamic viscosity (kg/ms) |
| $v$ | kinematic viscosity ($m^2/s$) |
| $\varepsilon_\tau$ | ratio of characteristic diffusion and acceleration times |
| $\rho$ | density ($kg/m^3$) |
| $\tau$ | characteristic time (s) |
| $\tau_a$ | gas acceleration characteristic time (s) |
| $\tau_\mu$ | radial viscous diffusion characteristic time (s) |

by the Dittus–Boetler equation. However, Webb and Zhang [8] found that their experimental results were adequately predicted by the commonly accepted correlations for single-phase flow in multiple tubes having hydraulic diameters between 0.96 and 2.1 mm. Wu and Little [9] measured the flow and heat transfer characteristics for the flow of nitrogen gas in heat exchangers, their reported Nusselt numbers for laminar flow ($Re < 600$) were lower than those predicted by traditional correlations. For $600 < Re < 1000 Nu$ was higher than the standard values. The laminar to turbulent heat transfer transition zone occurred at $Re$ ranging from 1000 to 3000. Mala and Li [10] measured the pressure drop and the flow rate for the flow of deionized water through microscale tubes with diameters ranging from 50 to 254 μm, the measured pressure gradient was much higher than the standard values, they found that the transition flow regime started at $Re = 650$.

## 2. Size effect mechanism

New questions have arisen in microscale flow and heat transfer. For example, the causes for the large differences existing in the reported friction factors and heat transfer coefficients and their physical mechanisms are still unexplained. These problems have been discussed in several review papers by Gad-el-Hak [11], Mehendale et al. [12], Darin et al. [13] and Palm [14]. It is commonly recognized that gas rarefaction leads to lower friction factors and Nusselt numbers for microscale gas flows. The review by Gad-el-Hak [11] focused on the physics related to the breakdown of the N–S equations. Besides the rarefaction effect, Mehendale et al. [12] noted that differences in the channel surface roughness could explain the disparities in the friction factors and the heat transfer data in some studies. They also thought that since the heat transfer coefficients were based on the inlet and/or outlet fluid temperatures, not the bulk temperature in almost all studies, comparison of conventional correlations is problematic. For the early transition from laminar to turbulent flow in microscale tubes, they pointed out that the thermophysical properties of the liquid change markedly as the fluid flows along the channel so that $Re$ at the channel exit could be twice that at the inlet. Therefore, the early transition to turbulence might be partially attributed to the variation in $Re$. Darin et al. [13] noted several effects that are improperly neglected when considering macroscale flow, for example, microscale phenomena may include two- or three-dimensional transport effects, and the temperature dependent variations of the transport fluid properties along a microchannel which may invalidate the often used assumption of constant properties, so that improved measurement accuracies are required to provide conclusive evidence of microscale effects. Palm [14] also

suggested possible explanations for the variations of microscale single-phase flow and heat transfer from conventional theory, including surface roughness effects, entrance effects, electric double-layer effects, non-constant fluid properties, two- and three-dimensional transport effects and the measurement accuracies.

Guo [15] classified the various mechanisms for the departure of flow and heat transfer correlations for flow in microchannels from the standard ones into two groups. First, if the characteristic length of the flow is on the same order of the magnitude as the molecular mean free path, the Navier–Stokes equations and the Fourier heat conduction equation break down and, consequently, the flow and heat transfer behaviors change considerably. This is the so-called rarefaction effect which can be represented by the Knudsen number, $Kn$, defined as the ratio of the molecular mean free path and the characteristic length of the flow. Secondly, the size effect on the flow and heat transfer correlations is attributed to the variation of the dominant factors in the flow and heat transfer as the scale decreases even though the continuum assumption is still applicable. For instance, forces exerted on the fluid which affect the flow and heat transfer whose effect on the convection changes at different scales, and axial heat conduction in the tube wall, which are commonly neglected for normal-sized devices, may become important at microscale. As a result, microscale flow and heat transfer correlations differ from those for normal-sized devices.

The assumption of a continuous flow is usually applicable for fluid flow in MEMS with hydraulic diameters more than tens of micrometers ($Kn \sim 0.001$) to $<1$ mm ($Kn \sim 0.0001$), gas rarefaction can thus be neglected. The present discussion will focus on the size effect induced by the variation of dominant factors in the flow and heat transfer as the device scale decreases. Since the surface to volume ratio is very large in microdevices, factors related to surface area will become more important. Some relevant related phenomena are the compressibility, the surface roughness, the variation of predominant forces and the surface geometry.

### 2.1. Flow compressibility effects

Gas flow in normal-sized tubes is usually assumed to be incompressible when the Mach number is much less than unity, so the gas density can be regarded as constant in the flow process. The flow in tubes becomes fully developed and the product of the friction factor and Reynolds number is equal to a constant if the tube length to diameter ratio is large enough. For flow in microtubes, there are only several theoretical studies dealing with the effect of the compressibility on the gas flow and the heat transfer. van der Berg et al. [16,17] solved the isothermal, compressible Navier–Stokes equations for laminar flow in a circular tube. For low Mach number flows, they obtained a local "self-similar" velocity profile with the product $f\,Re$ still equal to 64. Beskok et al. [18] numerically modeled the competing effects of compressibility and rarefaction for internal flows in long microchannels. Harley et al. [19] conducted an experimental and theoretical investigation of subsonic, compressible flow in microlong conduits, a one-dimensional (1-D) model was developed to evaluate the friction factor based on the locally fully developed approximation and to interpret the experimental data for low and moderate Mach number flow. Guo and Wu [20,21] found that the gas density variation in the flow direction might be very large if the surface friction induced pressure drop per tube length was much larger than that for conventional size tubes. Numerical solution of the governing equations for compressible flow in a circular tube gave the pressure and density variations along the tube for isothermal flow at different inlet Mach numbers shown in Fig. 1. The pressure variations were large near inlet even for an inlet Mach number, $M_0$, of 0.087 because the compressibility-induced gas acceleration and the increased momentum also contributed to the pressure decrease in addition to the friction. For compressible tube flow, the gas acceleration leads to the velocity profile changes not only in magnitude, but also in shape. The magnitude increments produce additional pressure drop, while the continuous variation in shape of the velocity profile means no fully or locally fully developed flow being occur. The numerical results for the compressibility effect on the friction factors are illustrated in Fig. 2.

Further analysis showed that the velocity profile in a uniform conduit is dependent on two factors for compressible flows: the axial gas acceleration and radial viscous diffusion of momentum, which can be characterized by their characteristic times, $\tau_a = (du_m/dx)^{-1}$ and $\tau_\mu = d^2/v$, where $u_m$ is the mean cross-sectional velocity of the gas flow. For a polytropic process, the ratio of the characteristic times of diffusion and acceleration, $\varepsilon_\tau$, can be approximated as

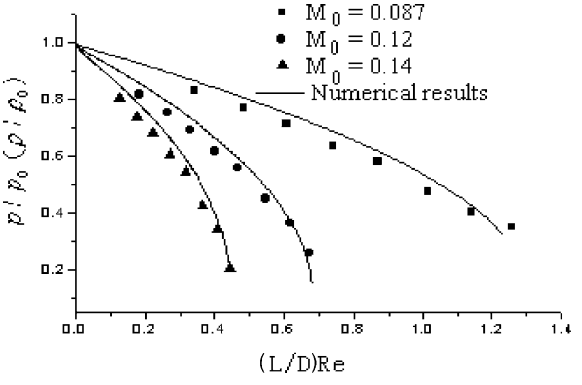


Fig. 1. Pressure and density variations along the flow direction.

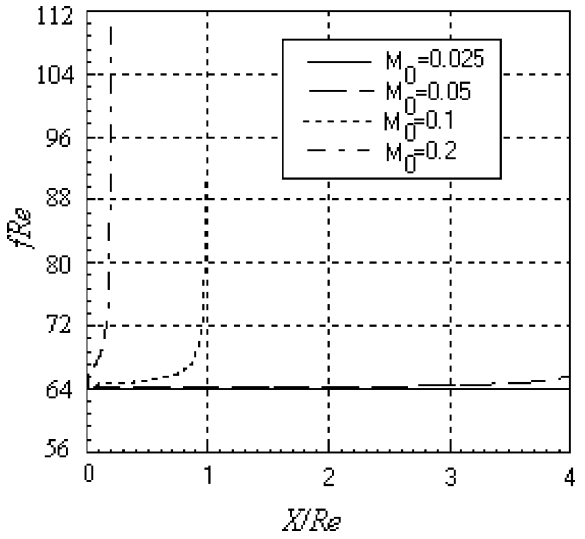


Fig. 2. Dependence of $f\,Re$ on location for various inlet Mach numbers.

$$\varepsilon_\tau = \tau_\mu/\tau_a = 8kM^2(x), \tag{1}$$

which represents the relative importance of diffusion and acceleration, i.e. the time ratio is a function of Mach number only. When $M(x) \ll 1$, $\varepsilon_\tau \ll 1$, that is the viscous diffusion process is much faster than the acceleration process, then the velocity profile remains parabolic as for incompressible flow in a circular tube. As long as the Mach number of the subsonic flow is not far from unity, the acceleration process dominates. As a result, as the gas flow downstream, the velocity profiles become much flatter than a parabolic distribution. Thus, fully developed gas flow does not occur in microtubes even for tubes with very large tube length to diameter ratio.

Assuming that the Mach number is not close to unity, the velocity, $u$, can be divided into two parts, $u = \bar{u} + \hat{u}$, where $\bar{u}$ is the parabolic one and $\hat{u}$ is the velocity component resulting from the flow compressibility. Their non-dimensional momentum equation were solved analytically to give the correlation for the friction factor [22],

$$f = \frac{64}{Re} + \frac{64}{Re}\frac{M^2}{1.5 - 0.66M - 1.14M^2}. \tag{2}$$

Li et al. [23] employed a tube-cutting method to measure the local pressures and local Mach numbers along a microtube. The experimental data and numerical results are shown in Figs. 1 and 3. The results again show that for flow in microtubes, the pressure variations are significant along the tube, and the local Mach number of the gas flow increases with increasing dimensionless distance from the inlet, and may become very large even for the small inlet Mach numbers. This phenomenon is critical for the design of microsystems since choking

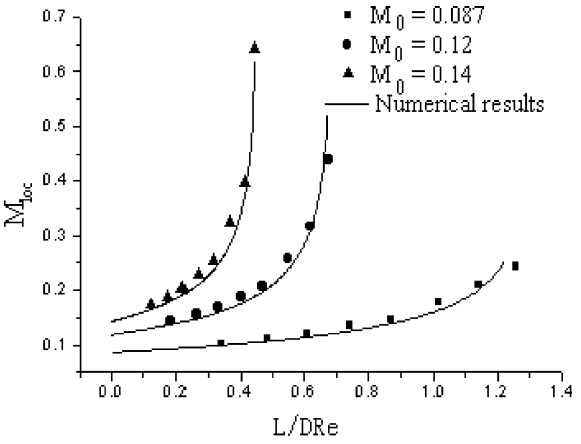


Fig. 3. Local Mach number variation along a microtube [23].

($M = 1$ at channel outlet) may occur in channel flows even for cases where the inlet Mach number is much smaller than unity. The characteristics of flow in microdevices was found to change from a cubic dependence to a linear dependence on the channel diameter for sonic flow in the channel, as mentioned by Jerman's work dealing with micromachined diaphragm valves [24].

The radial temperature profiles in the fluid are strongly dependent on the radial velocity profiles for tube flows. Therefore, no fully developed temperature profiles will occur as long as the flow is developing. Numerical results presented by Du [25] showed that the local Eckert numbers, like the friction factors, increase along the flow direction, as shown in Fig. 4. Furthermore, in view of the compressibility induced increase of Mach number, the Eckert number of the downstream flow may be rather large, even though the inlet Eckert number is small, as shown in Fig. 4. Therefore, the viscous dissipation and the work due to expansion cannot be neglected. The work due to expansion leads to

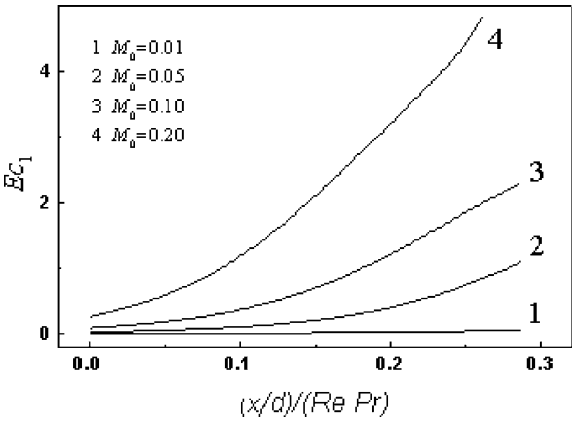


Fig. 4. Variation of Eckert number along the tube [25].

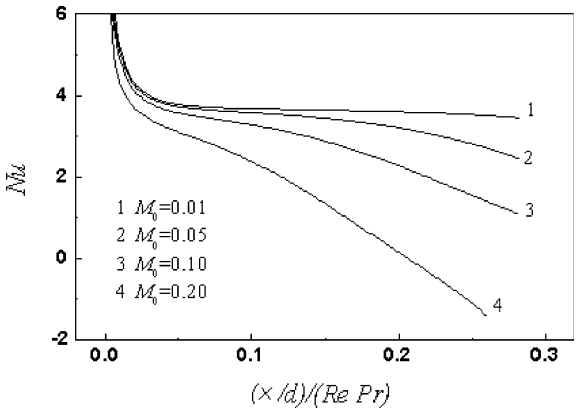


Fig. 5. Variation of Nusselt number along the tube.

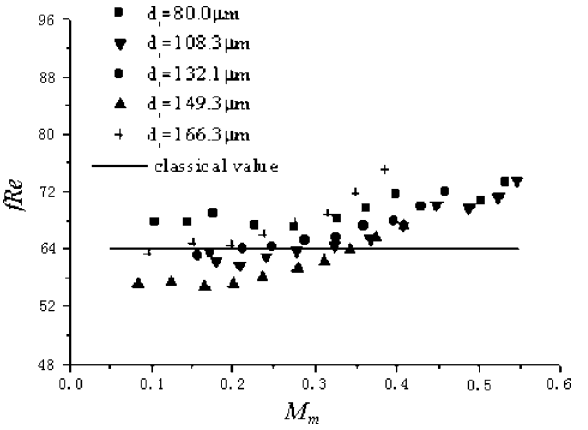


Fig. 6. Frictional factor for gas flow in smooth microtubes [15].

a gas temperature decrease in the channel interior, while the viscous dissipation results in a gas temperature rise in the near-wall region. The temperature rise in the near wall region leads to increased heat transfer. The conventionally defined Nusselt number may even be negative, as shown in Fig. 5 if the Mach number and the resulting consequent temperature decrease in the channel interior are large enough.

### 2.2. Effect of surface roughness

Only a few studies have considered the effect of roughness on laminar flow since Nikuradse (1933) [26] and Moody (1944) [27] concluded that the roughness effect on the laminar flow characteristics can be ignored if internal relative wall roughness is less than 5%. Some experimental and computational results for laminar flows have contradicted the Moody's well-known conclusion. Nikuradse's conclusion still pervades today because the flow in conventional-sized coarse tubes is usually turbulent, laminar flows being of less practical importance. However, flows in microchannels are often laminar, so the study of laminar flow in rough microchannels has become important.

The effect of channel size on the flow behavior was studied experimentally using water flow in smooth glass and silicon microchannels with diameters ranging from 80 to 166 μm [15]. The results show that the flow behavior is very similar to that for normal-sized channels, with the product of the Darcy friction factor and the Reynolds number, $f\,Re$, approximately a constant of 64 and the transition from laminar to turbulent flow beginning at around $Re = 2100$–$2300$. Experimental data for the friction factor for gas flow in smooth microchannels is shown in Fig. 6. Again, the friction factor is very similar to the standard value as long as the Mach number is $<0.3$, beyond that the increase in friction factor is caused by the flow compressibility.

Celeta et al. [28] measured the friction factor for R114 flowing in a channel 130 μm in diameter. The Reynolds number varied from 100 to 8000 and the relative channel surface roughness was 2.65%. Their experimental results show that for laminar flow, the friction factor was in good agreement with Hagen–Poiseuille theory for $Re < 583$; while for higher values of $Re$, the experimental data was higher than Hagen–Poiseuille theory; the transition from laminar to turbulent occurred for $Re$ in the range of 1881–2479. Wu and Little [1] estimated the friction factors for gas flow in trapezoidal microchannels with hydraulic diameters ranging from 30 to 60 μm and relative surface roughnesses between 0.05 and 0.30, they revealed that even for laminar flow the friction factor was influenced by the channel roughness. The experimental values for the friction factor normalized with respect to the theoretical values were found to vary from 1.3 to 3.5. They felt that their higher fraction factors were due to the variation of the flow cross-section caused by the large roughness. Mala and Li [10] measured the pressure drop and flow rate for the flow of deionized water through tubes with diameters ranging from 50 to 254 μm using stainless steel and fused silicon tubes with mean surface roughnesses between 0.007 and 0.035. Their results indicated significant departure of the flow characteristics for microtubes from the predictions of conventional theory. As the $Re$ increased, the measured pressure gradient was significantly higher than that predicted for Poiseuille flow. The variation of the friction factor, $f$, with $Re$ for microtubes from the data of Mala and Li [10] is shown in Fig. 7. They accounted for the measured roughness induced momentum transfer by introducing a roughness-viscosity analog to the concept of eddy viscosity in turbulent flow, and concluded that the measured friction was due to an early transition from laminar to turbulent flow and the increased surface roughness effect in microtubes.

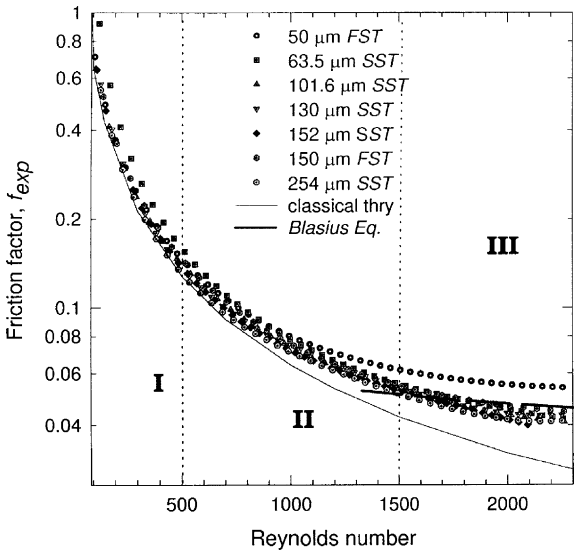


Fig. 7. Friction factor variation for microtubes [10].

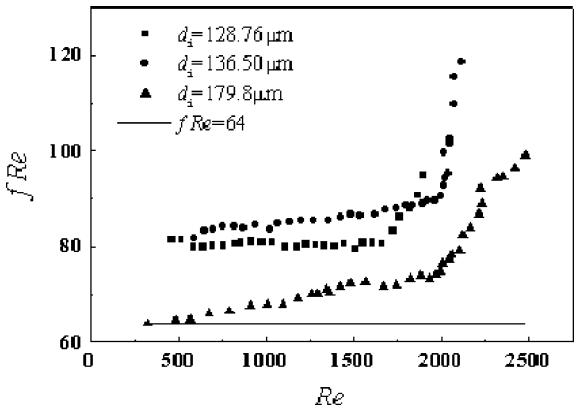


Fig. 8. Friction factor for rough microtubes [29].

Li et al. [23,29] conducted experiments to measure the pressure drop and the flow rate for laminar flow of deionized water through stainless steel microtubes with diameters of 128.8, 136.5 and 179.8 μm and relative surface roughnesses between 0.03 and 0.043. As shown in Fig. 8, the friction factors for these three cases were 10–25% higher than the theoretical values for *Re* between 500 and 2000. The transition from laminar to turbulent flow started at *Re* around 1800.

Du [25] numerical simulated laminar flow in rough microtubes to study the mechanism for the roughness effect. Based on a scanning electronic microscope (SEM) photo of the inner surface of a stainless steel microtube, regular three-dimensional roughness elements were used to simulate the roughness. The numerical results shown in Fig. 9 were in good agreement with the experimental

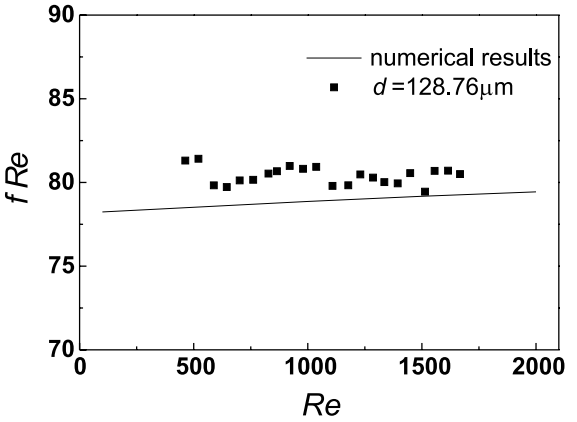


Fig. 9. Comparison of numerical and experimental friction factor results.

data. The numerical simulations show that the form drag resulting from the roughness elements is one reason leading to the increased friction factor. Another parameter which may affect the flow in microchannels is the roughness-generated flow disturbances. For a given relative roughness, the number of roughness elements per unit channel length is much larger for microchannels which would generate more frequent disturbances of the channel flow resulting in an increased friction factor. Finally, the disturbances will cause an early transition from laminar to turbulent flow when *Re* is large enough. In addition, since the turbulence is partly due to the roughness induced disturbances, rather than flow instabilities, the transition from laminar to turbulent might be continuous and smooth. Therefore, a surface roughness-viscosity model could be used to describe the increased friction factor and to understand the early transition to turbulence for fluid flow in microchannels.

### 2.3. Variation of predominate forces

Various kinds of forces may simultaneously act on a fluid flowing in a channel. For some flow and heat transfer problems, certain forces are important, while others may be neglected. Since different forces have different length dependences, as listed in Table 1, forces related to surfaces which are proportional to the length with a lower exponent (for example, the surface tension, the viscous force or the electrostatic force) become more

Table 1
Size effects of forces

| | | | |
|---|---|---|---|
| Electromagnetic force | $\sim L^4$ | Inertial force | $\sim L^2$ |
| Centrifugal force | $\sim L^4$ | Viscous force | $\sim L^1$ |
| Gravitational force | $\sim L^3$ | Surface tension | $\sim L^1$ |
| Buoyancy | $\sim L^3$ | Electrostatic force | $\sim L^{-2}$ |

important and even dominant as the object size is reduced.

Recently, Dao et al. [30] developed a novel accelerometer. The accelerometer is based on the free convection of a tiny hot air bubble in an enclosed chamber and does not require a solid proof mass, so it is compact, lightweight, and inexpensive to manufacture. Leung et al. [31] produced the device by bulk-silicon fabrication, and tests with natural gravity demonstrated that its sensitivity could reach 0.6 mg. Milanovic et al. [32] fabricated two kinds of convective accelerometers, thermopile and thermistor types using standard IC technology. Luo et al. [33] designed a micromachined convective accelerometer with a structure optimized for a bulk-silicon fabrication. The experimental data showed that the optimized device has better linearity, higher sensitivity and a preferable frequency response than other reported convective accelerometers.

The structure of the micromachined convective accelerometer proposed by Luo et al. [33] is shown in Fig. 10. It includes a cavity containing air as a working fluid, a heater about 80–100 μm in width and two temperature sensors. Air moves across the sensors by virtue of free convection. The device is packaged in a sealed chamber to prevent outside disturbances. When the electric heater is on, a free convection flow occurs in the cavity.

The temperature profile is symmetrical in the cavity when the accelerometer is not accelerating. There is no temperature difference between the two sensors if they are symmetric relative to the heater and the cavity if there is no convection in the axial direction due to acceleration. The acceleration modifies the free convection flow resulting in a skewed temperature field. The sensor can measure the acceleration since the temperature difference between the two sensors is directly related to the acceleration.

For natural convection around conventional-sized object, the buoyancy is largely balanced by the inertial force due to the small contribution of the viscous force. Since the inertial force is of the same order of magnitude as the buoyancy force, then

$$|U \cdot \nabla U| \sim |g\beta \Delta T| \quad \text{and} \quad U \sim (g\beta \Delta T)^{1/2}, \tag{3}$$

the ratio of the convection to conduction heat transfer is thus

$$|U \cdot \nabla T|/|a\nabla^2 T| \sim Ul/a \sim Gr^{1/2} Pr. \tag{4}$$

which leads to the well-known heat transfer correlation, $Nu \sim Gr^{1/4}$.

As the object size decreases, the viscous force dominates the inertial force at small Grashof numbers, and the viscous force balances the buoyancy force, i.e.

$$|v\nabla^2 U| \sim |g\beta \Delta T| \quad \text{and} \quad U \sim g\beta \Delta T l^3/v. \tag{5}$$

Therefore, the ratio of the convection to conduction heat transfer is then

$$|U \cdot \nabla T|/|a\nabla^2 T| \sim \mathrm{U1}/a \sim Gr\,Pr. \tag{6}$$

As a result, the heat transfer correlation will differ from that for natural convection on a infinite vertical plate. The numerical results of the relative magnitude of the forces for natural convection on a two-dimensional vertical plate with $Gr$ ranging from $10^0$ to $10^8$ are given in Fig. 11. The buoyancy is mainly balanced by the inertial force for $Gr$ from $10^6$ to $10^8$, while the inertial force can be neglected for $Gr$ from $10^1$ to $10^4$. Therefore, $Nu \sim Gr^{1/4}$ for $Gr$ from $10^6$ to $10^8$, while $Nu \sim Gr^{1/3}$ for $Gr$ from $10^1$ to $10^4$.

The heat transfer due to natural convection in a microenclosure can be divided into three regions as shown in Fig. 12. For $Ra > 10^6$, it is well known that $Nu \sim Ra^{0.33}$. For natural convection in a microenclosure with Ra ranging from $10^3$ to $10^6$, the inertial force is negligible, so $Nu \sim Ra^{0.284}$. If $Ra < 10^3$, the natural convection decrease towards zero so the heat transfer is only due to heat conduction as both the viscous and inertial forces can be neglected. However, the heat transfer may be underestimated if conventional heat transfer correlations are used for microscale natural convection, as indicated in Fig. 12 (see the dash line).

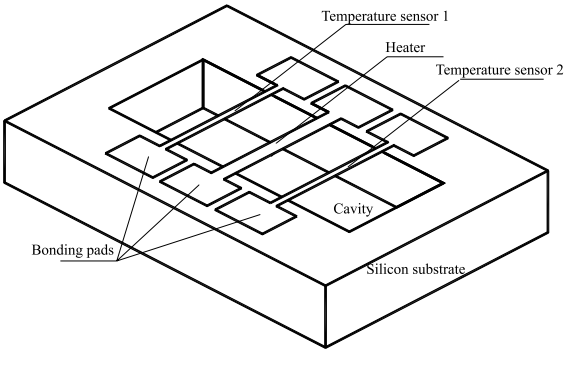


Fig. 10. Micromachined convective accelerometer [33].

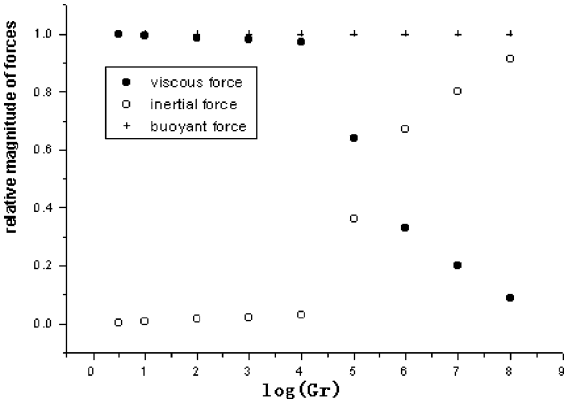


Fig. 11. Relative importance of inertial and viscous forces [15].

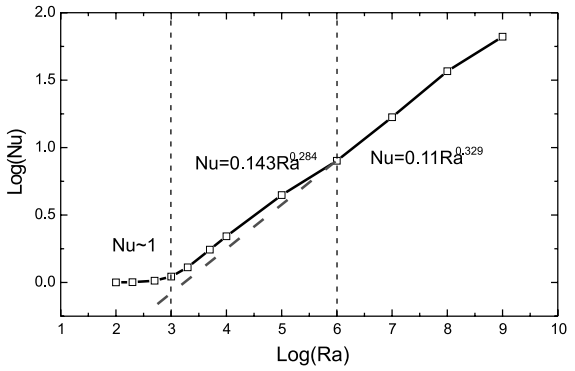


Fig. 12. Ratio of the inertial to viscous forces for flow in a square cavity.

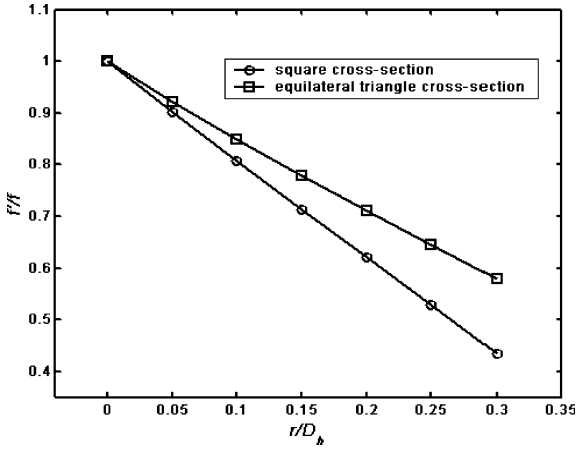


Fig. 13. Friction factors for liquid flows in square and equilateral triangle channels.

## 3. Variation of other predominant factors

### 3.1. Effect of surface geometry

The hydraulic diameter is commonly used to characterize the flow and heat transfer in non-circular conventional-sized tubes. For liquid flow in microchannels, dissolved gases in the liquid or gases absorbed on the surface may have considerable impact on the flow and heat transfer characteristics. As such gases collect in the corners of non-circular channels, the wetted perimeter will be reduced and the fluid velocity will increase as the actual flow cross-section is reduced. The smaller perimeter reduces the friction while the large velocity increases the friction. Square and equilateral triangle channels were analyzed numerically as examples.

The geometry and size of gas bubbles in the channel corners are dependent on the liquid surface tension and contact angle. Numerical results show that the wetted perimeter is more strongly dependent on the bubble size than the mean velocity. Hence, the friction decrease due to the reduced wetted perimeter will be larger than the friction increase due to the increased mean velocity.

The dependence of the normalized friction factor on the ratio of $r/D_h$ is illustrated for microchannels with square and equilateral triangle cross-sections in Fig. 13, where $r$ and $D_h$ are the arc radius and the channel hydraulic diameter. This dependence will differ for channels with different geometries. The dissolved gases come out of solution will reduce the measured friction factor. Smaller channel cross-sections will then have larger discrepancies between the experimental results for friction factor. Hence, the use of the hydraulic diameter is questionable for comparing correlations for liquid flow in microchannels with different geometries and for the same geometry with different sizes.

### 3.2. Effect of surface electrostatic charges

Most solid surfaces have electrostatic charges due to their electrical surface potential. If the liquid contains even very small amounts of ions, the electrostatic charges on the solid surface will attract the counterions in the liquid to establish an electrical field. The arrangement of the electrostatic charges on the solid surface and the balancing charges in the liquid is called the electrical double layer (EDL), which is usually very thin so its effect on the flow behaviors can be ignored. Mala et al. [34] investigated the interfacial electrokinetic effects on the liquid flow characteristics. They developed a mathematical model for steady liquid flow with consideration of the EDL effect. For solutions with high ionic concentrations, the EDL thickness was a few nanometers, while for infinitely diluted solutions, such as millipore water, the EDL thickness was up to 1 μm. In the latter cases, the EDL effect on the flow characteristics in microchannels becomes significant. The volume flow rates for millipore water in a 20 μm channel were significantly lower than that predicted by conventional fluid dynamics theory. In addition, the friction coefficient for flows in microchannels will increase as the zeta potential increases. Yang and Li [35] and Ren et al. [36] reported numerical and experimental results for the EDL effect with different liquids. They also found that the EDL effect led to a higher friction coefficient for pure water and dilute aqueous ionic solutions flowing in microchannels.

### 3.3. Effect of axial heat conduction in the channel wall

In general, the axial heat conduction in channel wall for conventional size channels can be neglected because the wall thickness is usually very small compared to the

channel diameter. Mori et al. [37] and Shah and London [38] found that the Nusselt number for developed laminar flow fall between 4.36 and 3.66, which correspond to Nusselt numbers for constant heat flux and constant temperature boundary conditions respectively. However, for flow in microchannels, the wall thickness can be of the same order of channel diameter will affect the flow and heat transfer in the microchannels.

The existing experimental results for heat transfer in microchannels differ significantly from that for conventional size channels. For example, Choi et al. [4] reported that the average Nusselt numbers in microchannels with hydraulic diameters from 9.7 to 81.2 μm were much lower than for standard channels and increased with increasing Reynolds number. Takano [39] obtained similar results for heat transfer in a circular microtube with an inner diameter of 52.9 μm and an outer diameter of 144.7 μm as also shown in Fig. 14. Both of Choi et al. [4] and Takano [39] applied a 1-D assumption to estimate the overall thermal resistance from the outer wall or fluid to the fluid in the channel. Note that the 1-D assumption may be invalid for estimating the overall thermal resistance in microchannels. As for example, a numerical solution [39] of the conjugated heat transfer problems showed that the Nusselt number for flow in microchannels is around a constant value, rather than a function of Reynolds number (Fig. 15). For comparison, we used 1-D model to calculate the heat transfer coefficient for water flow in microchannels with different channel thickness to diameter ratios or different ratio of outer to inner diameter, $R^*$. The results shown in Fig. 15 have similar trends with the experimental data from Takano [39]. Nusselt numbers are much lower than the predicted constant value [39] and increase with increasing $Re$. These results indicate that the 1-D model for the thermal resistance based on the assumption of no axial heat conduction in the channel wall causes the experimental results for $Nu$ to be less than the standard values.

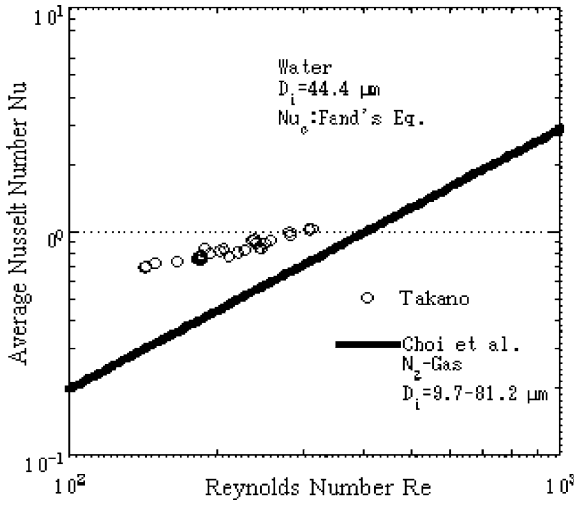


Fig. 14. Nusselt number variation for microchannels [39].

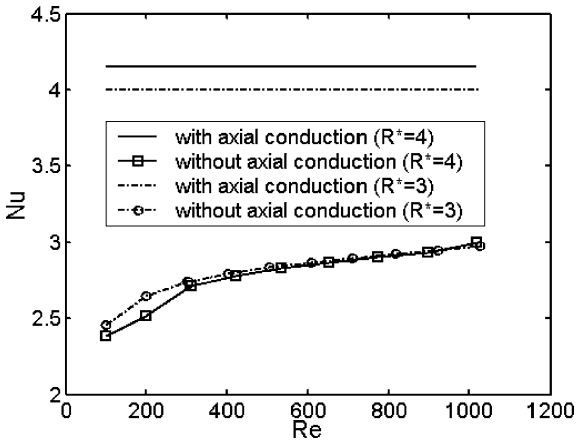


Fig. 15. Effect of the axial heat conduction in the channel wall.

### 3.4. Effect of measurement accuracy

In the experiments of flow and heat transfer in microchannels, some parameters, such as the flow rate and channel dimensions are difficult to measure accurately because they are very small. For example, the relative error of the measured channel height reported by Pfahler et al. [40] was up to 20%.

In our experiments for measuring the flow resistance in a circular glass microtube, we initially measured the diameter as 84.7 μm using a 40× microscope. The data reduction with this measured diameter showed that the friction factors were larger than that predicted by conventional theory. The average value of the diameter measured using a 400× microscope and a SEM for the same microtube was only 80.0 μm. With this more accurate value of the diameter, the frictional factors obtained from the experimental data were in good agreement with the conventional values.

For single-phase flow in microchannels, Palm [14] suggested that some of the deviations in the experimental results may be caused by the difficulties in accurately determining the hydraulic diameters. Du et al. [14] carried out an uncertainty analysis of the Darcy equation for incompressible flow in circular channel flows. The uncertainty of $f\,Re$ is

$$\frac{\delta(f\,Re)}{(f\,Re)} = \left\{ \left( \frac{\delta(\Delta p)}{\Delta p} \right)^2 + \left( 4\frac{\delta d}{d} \right)^2 + \left( \frac{\delta l}{l} \right)^2 + \left( \frac{\delta m}{m} \right)^2 \right\}^{1/2} \tag{7}$$

where $m$, $\Delta p$, $d$, $l$ are respectively the mass flow rate, pressure drop, tube diameter and tube length. Eq. (7)

shows that the tube diameter measurement error may play a very important part in the uncertainty of the friction factor, $f\,Re$. The discrepancies among different friction factor and heat transfer correlations proposed by various investigators may be, at least in part, attributed to the uncertainties of the experimental data.

## 4. Concluding remarks

(1) The physical mechanisms for the size effect on the microchannel flow and heat transfer can be divided into two classifications: (a) The gas rarefaction effect occurs when the continuum assumption breaks down as the characteristic length of the flow becomes comparable to the mean free path of the molecules. (b) Variations of the predominant factors influence the relative importance of various phenomena on the flow and heat transfer as the characteristic length decrease, even if the continuum assumption is still valid.

(2) Since the characteristic lengths of flows in MEMS are from tens of micrometer ($Kn \sim 0.001$) to fractions of 1 mm ($Kn \sim 0.0001$), in most cases the assumption of flow continuum is usually valid. Hence, the size effect on the flow and heat transfer in MEMS should be largely attributed to the variation of the predominant factors or phenomena in the flow and heat transfer processes.

Because the microdevices have a large surface to volume ratio, factors related to surface effects have more impact to the flow and heat transfer at small scales. Among these are: (a) surface friction induced flow compressibility, which makes the fluid velocity profiles flatter and leads to higher friction factors and Nusselt numbers; (b) surface roughness, which is likely responsible for the early transition from laminar to turbulent flow and the increased friction factor and Nusselt number; (c) the importance of viscous force in natural convection, which modifies the correlation between $Nu$ and $Ra$ for natural convection in a microenclosure; and (d) other effects, which include channel surface geometry, surface electrostatic charges, axial heat conduction in the channel wall and measurement errors. All these factors may cause the flow and heat transfer behavior in microchannels differ from that at conventional scales.

(3) Discrepancies between experimental results for the friction factor and the Nusselt number and their standard values due to the measurement errors might be misunderstood as being caused by novel phenomena at microscales.

## Acknowledgement

The project was financially supported by the National Natural Science Foundation of China with Grant number 59995550-2.

## References

[1] P.Y. Wu, W.A. Little, Measurement of friction factors for the flow of gases in very fine channels used for microminiature Joule–Thomson refrigerators, Cryogenics 23 (1983) 273–277.
[2] J. Pfahler, J. Harley, H. Bau, Liquid and gas transport in small channels, ASME DSC-19 (1990) 149–157.
[3] J. Pfahler, J. Harley, H. Bau, Gas and liquid flow in small channels, ASME DSC-32 (1991) 49–60.
[4] S.B. Choi, R.F. Barron, R.Q. Warrington, Fluid flow and heat transfer in micro tubes, ASME DSC-32 (1991) 123–133.
[5] I. Papautsky, J. Brazzle, T. Ameel, A.B. Frazier, Laminar fluid behavior in microchannels using micropolar fluid theory, Sensors Actuat. 73 (1999) 101–108.
[6] I. Papautsky, B.K. Gale, S. Mohanty, T.A. Ameel, A.B. Frazier, Effects of rectangular microchannel aspect ratio on laminar friction constant, Proc. SPIE Microfluidic Dev. Syst. II 3877 (1999) 147–158.
[7] B.X. Wang, X.F. Peng, Experimental investigation of liquid forced-convection heat transfer through microchannels, Int. J. Heat Mass Transfer 37 (1994) 73–82.
[8] R.L. Webb, M. Zhang, Heat transfer and friction in small diameter channels, Microscale Thermophys. Eng. 2 (1998) 189–202.
[9] P.Y. Wu, W.A. Little, Measurement of the heat transfer characteristics of gas flow in fine channel heat exchangers used for microminiature refrigerators, Cryogenics 24 (1984) 415–420.
[10] G.M. Mala, D. Li, Flow characteristics of water in microtubes, Int. J. Heat Fluid Flow 20 (1999) 142–148.
[11] M. Gad-el-Hak, The fluid mechanics of microdevices, Based on the 14 Freeman Lecture, ASME/WAM.
[12] S.S. Mehendale, A.M. Jacobi, R.K. Shah, Heat exchangers at micro- and meso-scales, Proc. Int. Conf. Compact Heat Exchangers and Enhance Technology for the Process Industries, Banff, Canada, 1999, pp. 55–74.
[13] K. Drain et al., Single phase forced convection heat transfer in microgeometries—A review, Proc. 30th Intersociety Energy Conversion Engineering Conference, Florida, 1995.
[14] R. Palm, Heat transfer in microchannels, Microscale Thermophy. Eng. 5 (3) (2001) 155–175.
[15] Z.Y. Guo, Characteristics of microscale fluid flow and heat transfer I MEMS, Proc. Int. Conf. Heat Transfer and Transport Phenomena in Microscale, Banff, Canada, 2000, pp. 24–31.
[16] R.H. van der Berg, C.A. Seldam, P.S. ven der Gulik, Compressible laminar flow in a capillary, J. Fluid Mech. 246 (1993) 1–20.
[17] R.H. vanderBerg, C.A. Seldam, P.S. ven der Gulik, Thermal effects in compressible viscous flow in a capillary, Int. J. Thermophys. 14 (1993) 865–892.
[18] A. Beskok, E.K. George, T. William, Rarefaction and compressibility effects in gas microflows, ASME J. Fluid Eng. 118 (1996) 448–456.
[19] J. Harley, Y. Huang, H. Bau, J. Zemel, Gas flow in microchannel, J. Fluid Mech. 284 (1995) 257–274.
[20] Z.Y. Guo, X.B. Wu, Compressibility effect on the gas flow and heat transfer in a micro tube, Int. J. Heat Mass Transfer 40 (1997) 3251–3254.

[21] Z.Y. Guo, X.B. Wu, Further study on compressibility effect on the gas flow and heat transfer in a microtube, Microscale Thermophys. Eng. 2 (1998) 111–120.
[22] Z.X. Li, Z.Z. Xia, D.X. Du, Analytical and experimental investigation on gas flow in a microtube, Kyoto University–Tsinghua University Joint Conference on Energy and Environment, Kyoto, Japan, November 1999, pp. 1–6.
[23] Z.X. Li, D.X. Du, Z.Y. Guo, Investigation on the characteristics of frictional resistance of gas flow in microtubes, Proc. Symposium on Energy Engineering in the 21st Century, vol. 2, 2000, pp. 658–664.
[24] J.H. Jerman, Electrically-activated, micromachined diaphragm valves, IEEE Solid-State Sensor and Actuator Workshop June 4–7 1990, Sponsored by: IEEE Electron Devices Soc., Publ. by IEEE, pp. 65–69.
[25] D.X. Du, Effect of compressibility and roughness on flow and heat transfer in microtubes, Doctoral degree thesis, Tsinghua University, 2000 (in Chinese).
[26] J. Nikuradse, Strmungsgesetze in rauhen rohren, V.D.I. Forschungsheft 361 (1933) 1–22.
[27] L.F. Moody, Friction factors for pipe flow, Trans. ASME 66 (1944) 671–684.
[28] G.P. Celata, M. Cumo, M. Gulielmi, G. Zummo, Experimental investigation of hydraulic and single phase heat transfer in 0.130 mm capillary tube, in: G.P. Celata et al. (Eds.), Proc. Int. Conf. Heat Transfer and Transport Phenomena in Microscale, Begell House, Inc., New York, Wallingford, UK, 2000, pp. 08–113.
[29] Z.X. Li, D.X. Du, Z.Y. Guo, Experimental study on flow characteristics of liquid in circular microtubes, Proceedings of the International conference on Heat Transfer and Transport Phenomena in Microscale, Banff, Canada, 2000, pp.162–167.
[30] R. Dao, D.E. Morgan, H.H. Kries, D.M. Bachelder, Convective accelerometer and inclinometer, United States Patent 5581034, 1996.
[31] A.M. Leung, J. Jones, E. Czyzewska, J. Chen, M. Pascal, Micromachined accelerometer with no proof mass, Tech. Digest Int. Electron Dev. Meeting (1997) 899–902.
[32] V. Milanovic, E. Bowen, M.E. Zaghloul, et al., Micromachined convective accelerometers in standard integrated circuits technology, Appl. Phys. Lett. 76 (4) (2000) 508–510.
[33] X.B. Luo, Y.J. Yang, Z. Zhang, Z.X. Li, Z.Y. Guo, An optimized micromachined convective accelerometer with no proof mass, J. Micromech. Microeng. 11 (2001) 504–508.
[34] G.M. Mala, D. Li, C. Werner, et al., Flow characteristics of water through a microchannel between two parallel plates with electrokinetic effects, Int. J. Heat Fluid Flow 18 (5) (1997) 491–496.
[35] C. Yang, D. Li, Analysis of electrokinetic effects on the liquid flow in rectangular microchannels, Coll. Surf. A: Physicochem. Eng. Aspects 143 (1998) 339–353.
[36] L. Ren, W. Qu, D. Li, Interfacial electrokinetic effects on liquid flow in microchannels, Int. J. Heat Mass transfer 44 (2001) 3125–3134.
[37] S. Mori, M. Sakakibara, A. Tanimoto, Steady heat transfer to laminar flow in a circular tube with conduction in tube wall, Heat Transfer—Jpn. Res. 3 (2) (1974) 37–46.
[38] R.K. Shah, A.L. London, Laminar flow forced convection in ducts, in: T.F. Irvine, J.P. Hartnett (Eds.), Advances in Heat Transfer, Supplement 1, Academic Press, New York, San Francisco, London, 1978.
[39] K. Takano, Personal correspondence, June 19, 2001.
[40] J. Pfahler, J. Harley, H. Bau, Liquid transport in micron and submicron channels, Sensors Actuat. A21–A23 (1990) 431–434.